

# TF-Mamba: A Time-Frequency Network for Sound Source Localization

Yang Xiao and Rohan Kumar Das  
Fortemedia Singapore, Singapore  
Email: {xiaoyang, rohankd}@fortemedia.com

**Abstract**—Sound source localization (SSL) determines the position of sound sources using multi-channel audio data. It is commonly used to improve speech enhancement and separation. Extracting spatial features is crucial for SSL, especially in challenging acoustic environments. Previous studies performed well based on long short-term memory models. Recently, a novel scalable SSM referred to as Mamba demonstrated notable performance across various sequence-based modalities, including audio and speech. This study introduces the Mamba for SSL tasks. We consider the Mamba-based model to analyze spatial features from speech signals by fusing both time and frequency features, and we develop an SSL system called TF-Mamba. This system integrates time and frequency fusion, with Bidirectional Mamba managing both time-wise and frequency-wise processing. We conduct the experiments on the simulated dataset and the LOCATA dataset. Experiments show that TF-Mamba significantly outperforms other advanced methods on simulated and real-world data.

**Index Terms**—DOA Estimation, Sound Source Localization, Mamba, State-space Model

## I. INTRODUCTION

Sound source localization (SSL) [1] aims to automatically identify the origins of sound by analyzing signals captured through a microphone array. The core functionality of SSL systems is to calculate the angles at which sounds reach the microphones. This spatial information is essential for many speech-based applications, including speech separation [2]–[4], speech recognition [5], and speech enhancement [6]. Accurate sound localization can assist these applications to improve their performance. As a result, developing more advanced SSL techniques has become a key focus in research, aiming for greater robustness and adaptability in real-world.

Traditional SSL methods estimate spatial features linked to direct-path signal propagation to map features to source locations. Common spatial features include time delay, inter-channel phase/level difference (IPD/ILD) [7], and relative transfer function (RTF) [8]. For example, the steered response power (SRP) based methods, particularly SRP-PHAT [9], which is obtained from the SRP by applying phase transform whitening, have been foundational due to their simplicity and versatility. These spatial features are easy to estimate in ideal conditions but become challenging in real-world scenarios with noise, reverberation, and multiple moving sources. Because the noise and overlapping speech cause distortions, while reverberation masks or colors the signal. Additionally, moving sources create time-varying spatial cues, also leading to a significant decline in localization accuracy.

In recent years, deep learning methods for localization have gained more attention [10]–[12] than traditional methods. These methods approach the task as either feature/location regression or location classification. Common architectures for moving SSL include convolutional neural networks (CNNs) [13], [14] and recurrent neural networks (RNNs) [15], [16]. CNNs extract local spatial features, while RNNs capture long-term temporal context. Deep learning models can take input at the signal level (e.g., time-domain signals, spectrograms) or feature level (e.g., inter-channel phase difference, generalized cross-correlation (GCC) [17], spatial spectrum). Motivated by speech enhancement, the FN-SSL [18] framework builds on previous work, recognizes that the direct-path inter-channel phase difference can be estimated in both narrow-band (frequencies) and full-band (time-frames). It uses dedicated LSTM layers to process each band and show advanced performance.

While LSTM-based models like FN-SSL have shown promising results, a new neural state space model (SSM)-based architecture called Mamba [19], [20] has emerged and achieves superior performance to state-of-the-art models across various tasks [21], [22]. In speech processing, there have been attempts to replace transformers and RNNs with Mamba for tasks like speech separation and speech enhancement [23]–[25]. Mamba demonstrates a stronger ability to model extremely long-range dependencies compared to LSTM and is notable for its efficient use of computational resources.

In this work, we *introduce Mamba to SSL* by proposing a novel architecture referred to as TF-Mamba. It is built on the robust FN-SSL framework, which uses LSTM for time and frequency feature fusion. By replacing the LSTM blocks in FN-SSL with bidirectional Mamba (BiMamba) blocks, TF-Mamba aims to improve audio sequence context modeling while maintaining linear complexity with sequence length. We consider both simulated and LOCATA datasets for our studies to evaluate the effectiveness of proposed TF-Mamba for real-world scenarios. To the best of our knowledge, this is the first attempt to use a state-space-based model for SSL.

## II. RELATED WORKS

### A. Mamba for Speech

Mamba has demonstrated transformer-level performance across various sequence-based modalities, including audio and speech, which are naturally sequential in waveform or spectrogram forms. Early works applied Mamba to single

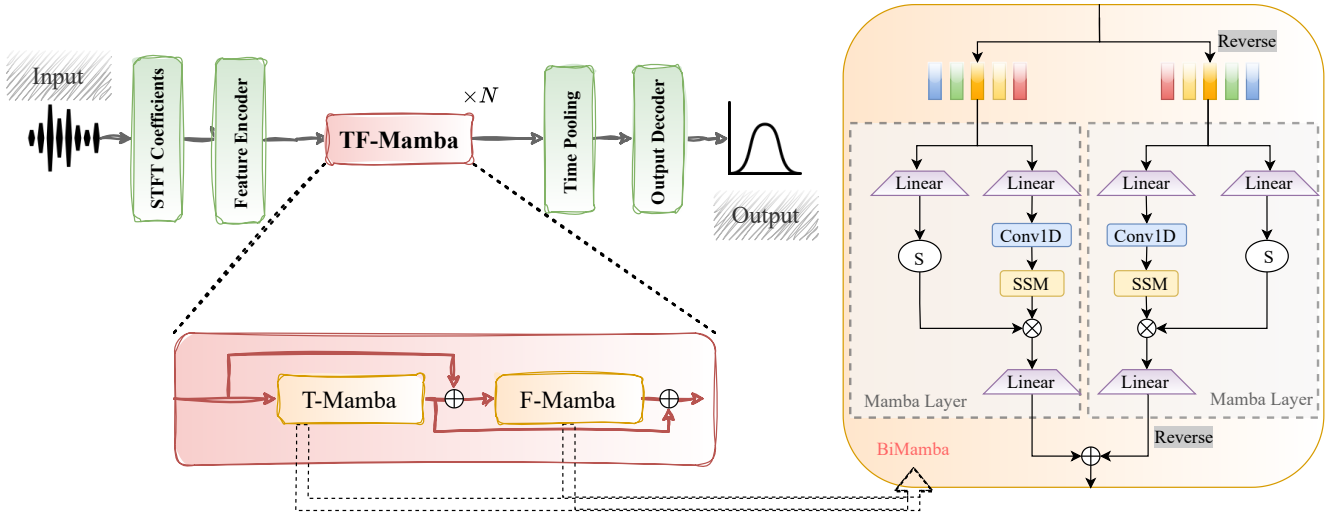


Fig. 1. Architecture of the proposed TF-Mamba network. Each TF-Mamba block includes a temporal Mamba (T-Mamba) and frequency Mamba (F-Mamba) layer, with skip connections to prevent information loss. Bidirectional Mamba (BiMamba) layers capture both past and future information. “S” denotes the SiLU activation and “Linear” indicates linear projection.

tasks such as speech enhancement [25], [26], speech separation [23], [24], and audio detection and classification [27], [28]. Additionally, some studies explored self-supervised audio transformers trained with masked spectrogram modeling [29]. The most comprehensive studies to date examine Mamba’s applications in speech enhancement, recognition, synthesis, understanding, and summarization. However, effective model design using SSMs for deep SSL remains unexplored.

### B. Deep Sound Source Localization

In recent years, significant progress has been made in SSL using neural networks. Cross3D [30] uses the SRP-PHAT spatial spectrum as input and employs a causal 3D CNN network for tracking moving sound sources. Similarly, SE-ResNet [31] utilizes a squeeze-and-excitation residual network as an encoder and a gated recurrent unit (GRU) network as a decoder. While SELDnet [32] takes frequency-normalized inter-channel phase difference (IPD) concatenated with the magnitude spectrum as input, SALSALite [33], similar to SELDnet, uses frequency-normalized IPD with the magnitude spectrum as input and a ResNet-GRU network. With advanced performance, the FN-SSL [18] also uses direct path IPD as input and leverages dedicated full-band and narrow-band LSTM layers to exploit inter-band dependencies and inter-channel information.

## III. PROPOSED TF-MAMBA

### A. Mamba

The structured SSMs [19], [20] efficiently handles long-dependent sequences with low computation and memory needs, serving as a substitute for transformers or RNNs. Mamba [34] enhances SSM by introducing an input-dependent selection mechanism for efficient information filtering and a hardware-aware algorithm that scales linearly with sequence

length, enabling faster computation. Mamba’s architecture, combining SSM blocks with linear layers, is simpler but achieves state-of-the-art performance across various long-sequence tasks, offering significant computational efficiency during both training and inference.

The core of Mamba is a linear selective SSM. In the equation below, the variables  $h_t$ ,  $x_t$ , and  $y_t$  represent the hidden state, input, and output at time  $t$ , respectively. The matrices  $A$ ,  $B$ , and  $C$  are learnable parameters corresponding to the state transition, input, and output processes.

$$h_t = Ah_{t-1} + Bx_t, \quad y_t = Ch_t \quad (1)$$

Due to its linear nature, the entire output sequence  $y$  of length  $\mathcal{L}$  can be expressed as a convolution between the input sequence  $x$  of the same length and a kernel  $\mathcal{K}$ .

$$y = x * \mathcal{K}, \quad \text{where } \mathcal{K} = (CB, AB, \dots, CA^{\mathcal{L}-1}B) \quad (2)$$

Since the matrices  $A_t$ ,  $B_t$ , and  $C_t$  depend on the input  $x_t$  (i.e., they are selective), this convolution cannot be computed directly but is instead solved using a parallel scan algorithm. A unidirectional Mamba is an SSM positioned between gated linear layers. For most speech-related tasks, bidirectional modeling is preferred because it captures information from both past and future sequences. Therefore, we use the bidirectional Mamba (BiMamba) proposed in [25], where two SSMs and causal convolutions run in parallel: one processes the original sequence, and the other processes the reversed sequence. The outputs from both SSMs are averaged to incorporate information from both directions.

### B. Network Architecture

The structure of the proposed TF-Mamba network is illustrated in Fig. 1. The input to the network consists of the real

and imaginary parts of the STFT coefficients, resulting in an input channel count that is twice the number of microphones. The model has three modules as follows:

1) *Feature Encoder*: The inputs are first processed by a feature encoder, which consists of a dilated DenseNet [35] core flanked by two convolutional layers to enhance its spectral properties. The output from the feature encoder is then transformed through the Time-Frequency Mamba block.

2) *Time-Frequency Mamba*: The Time-Frequency Mamba (TF-Mamba) block consists of one temporal Mamba layer and one frequency Mamba layer. Fig. 1 illustrates a network with a TF-Mamba block, with additional blocks easily added by repeating the block multiple ( $N$ ) times.

**The temporal Mamba layers** process time frames independently, with all frames sharing the same network parameters. The input is a sequence along the frequency axis of a single time frame, allowing the temporal Mamba layers to learn inter-frequency dependencies related to spatial and localization cues. These layers do not capture temporal information, which is instead handled by the subsequent frequency Mamba layers.

**The frequency Mamba layers** process frequencies independently, with all frequencies also sharing parameters. Differing from the temporal Mamba, the input is a sequence along the time axis of a single frequency, where the frequency Mamba layers estimate direct-path localization features. Estimating these features frequency-wise has been extensively studied in conventional methods such as in [18]. The proposed frequency Mamba layers focus on exploiting this inter-channel information. Additionally, since it is time-varying for moving sound sources, the frequency Mamba layers also learn the temporal evolution of the direct-path localization features.

Mamba is useful because it efficiently models long-range dependencies while maintaining computational efficiency. The ability of Mamba to handle both temporal and frequency-specific features in a structured manner makes it ideal for capturing complex relationships in audio data, such as the time-varying nature of localization cues, which are crucial for accurate SSL. However, the temporal Mamba and frequency Mamba layers are designed to focus on their respective types of information. Therefore the pieces of information from the frequency Mamba layer can be lost after passing through a temporal Mamba layer, and vice versa. To prevent this information loss, we add skip connections. As shown in Fig. 1, the output of each temporal Mamba layer is added to the input of the following temporal Mamba layer. Similarly, the output of each frequency Mamba layer is added to the input of the next frequency Mamba layer. Further, each Mamba layer inside BiMamba also has the skip connection.

3) *Output Decoder*: The output from the TF-Mamba blocks is then passed through an average pooling module to reduce the frame rate and is subsequently fed into a fully connected layer with tanh activation, which converts the output to the desired dimension. We employ a spatial spectrum prediction module for DOA estimation as in [36]. This system learns complex relationships from the audio data to predict the potential origin of sound at every degree within a half-circle

of the linear microphone array. The resulting spatial spectrum is an 181-point map. We train our model by minimizing the mean squared error (MSE) loss between the model’s output spatial spectrum and the ground truth.

## IV. EXPERIMENT SETTING

### A. Datasets

We evaluated the proposed method on both simulated and real-world datasets, using two microphones to localize the direction of arrival (DOA) within a 180-degree azimuth range.

**Simulated dataset**: Microphone signals are obtained by convolving room impulse responses (RIRs) with speech source signals [12]. The speech signals are randomly selected from the training, development, and test sets of the LibriSpeech corpus [37], and then used for model training, validation, and testing, respectively. RIRs are generated using the `gpuRIR` [38]. We followed the settings from [18] to obtain the simulated dataset with moving sources. The room reverberation time (RT60) is randomly set between 0.2 and 0.6 seconds, and the room size ranges from  $4 \times 2 \times 2$  m to  $10 \times 8 \times 5$  m. The moving trajectories of speech sources are generated according to [30], with each source maintaining a fixed height. Two microphones, placed 8 cm apart, are randomly positioned in the room on the same horizontal plane as the sound source. This dataset includes 1,511 audio files, which amount to approximately 4.96 hours of speech data. Based on the RIRs, we generate the mixture data for each original single-channel speech data for every 5 degrees from 0 to 180 degrees, which expands the audio files by 37 times. We then use white, babble, and factory noises from the NOISEX-92 [39] dataset as noise sources and create a diffuse sound field described in [40]. The generated diffuse noise signals are added to the clean signals with a signal-to-noise ratio (SNR) between -10 and 10 dB for noise robustness.

**Real-world dataset**: We also tested our proposed method on tasks 3 and 5 of the LOCATA dataset [41] following the setting in [18]. The room size was  $7.1 \times 9.8 \times 3$  m, with a reverberation time of 0.55 s. We used microphones 6 and 9 from the DICIT array [42], which have the same configuration as the simulated microphone array. The models trained on the simulated dataset were directly tested on the LOCATA dataset.

### B. Implementation details and metrics

For training each task with our proposed TF-Mamba model, we use 100 epochs with a 20-epoch early stopping criterion. We utilize the AdamW optimizer with a learning rate of 0.001. Additionally, we employ StepLR, to adjust the learning rate during training. For STFT computations, the frame size is set to 32 milliseconds, and the hop size to 10 milliseconds. The frequency range for the STFT is between 100 Hz and 8000 Hz, with an `n_fft` value of 512, which determines the length of the windowed signal after zero-padding.

We use two primary metrics: mean absolute error (MAE) and accuracy (ACC). MAE quantifies the average magnitude of prediction errors, disregarding their direction. ACC, on the other hand, measures the percentage of predictions that

TABLE I

ABLATION STUDIES OF TF-MAMBA ON SIMULATED DATA. “EXPAND” DENOTES THE EXPAND FACTOR FOR THE MAMBA LAYER.

Components	Params[M]	ACC(15°) [%]	ACC(10°) [%]	MAE [°]
Block $\times$ 3 (Expand = [2,2,2])	0.9	96.5	92.6	2.89
Block $\times$ 4 (Expand = [2,2,4,4])	1.3	98.4	94.9	2.87
Block $\times$ 5 (Expand = [2,2,4,4,8])	1.8	<b>98.9</b>	<b>96.9</b>	<b>2.52</b>
w/o BiMamba	1.4	97.1	93.6	2.84
w/o Skip	1.8	97.9	95.4	2.65

TABLE II

PERFORMANCE COMPARISON IN ACC AND MAE ON SIMULATED DATA.

Methods	Params [M]	Clean			-10 dB		
		ACC(15°)	ACC(10°)	MAE[°]	ACC(15°)	ACC(10°)	MAE[°]
SELDnet	0.8	96.6	93.8	3.5	52.8	50.2	16.7
FN-SSL	2.1	98.3	95.9	2.8	71.6	68.4	8.9
Cross3D	5.6	84.8	81.3	6.5	38.8	35.4	26.3
SE-ResNet	10.2	96.7	95.1	3.2	67.7	64.6	10.8
SALSA-Lite	14.0	96.8	95.6	2.9	69.1	65.7	10.3
TF-Mamba	1.8	<b>98.9</b>	<b>96.9</b>	<b>2.5</b>	<b>74.6</b>	<b>72.5</b>	<b>8.2</b>

are exactly correct or within a specified tolerance. We assess accuracy at two tolerance levels: within a 10° and 15° error margin. These tolerance levels provide insight into the model’s precision as well as its practical effectiveness.

### C. Reference baselines

We compared the following five moving SSL methods: Cross3D [30], SELDnet [32], SE-Resnet [31], SALSA-Lite [33], and FN-SSL [18]. It is noted that the SELDnet, SALSA-Lite, and SE-ResNet are models designed for joint sound event detection and localization; hence, we only utilize their localization branches for comparison. All these methods are reproduced and trained on the same dataset as our proposed method. We adjust the time pooling kernel size in each method to achieve the same output frame rate across all models for consistency.

## V. RESULTS AND ANALYSIS

### A. Ablation: Finding the best configuration for TF-Mamba

The ablation study results for TF-Mamba, shown in Table I, highlight the importance of different components in the network. “Block  $\times$   $N$ ” refers to stacking  $N$  number of TF-Mamba blocks. As the number of blocks increases from 3 to 5, accuracy (10° error tolerances) improves from 92.6% to 96.9%, showing that deeper networks help the model understand more complex localization information. The “w/o BiMamba” variant, which replaces the bidirectional mamba with unidirectional, reduces accuracy to 93.6% (10°) and 97.1% (15°). This shows that processing both past and future information is important for achieving good performance. The “w/o Skip” variant, which excludes skip connections, also leads to a small drop in accuracy and a higher error. This confirms that skip connections are helpful in keeping information flowing through the network. We use Block  $\times$  5 version with BiMamba and skip connections in the following comparison experiments.

### B. Results on simulated data

We report the results in two acoustic conditions of testing in Table II which are “Clean” and “SNR=-10 dB”. The results demonstrate that TF-Mamba outperforms other methods in

TABLE III

PERFORMANCE COMPARISON IN ACC AND MAE ON LOCATA DATASET.

Methods	Params[M]	ACC(15°)	ACC(10°)	MAE [°]
SELDnet	0.8	94.1	91.2	5.3
FN-SSL	2.1	96.7	93.3	3.6
Cross3D	5.6	94.8	91.4	5.1
SE-ResNet	10.2	94.0	90.7	6.5
SALSA-Lite	14.0	95.0	92.5	4.6
TF-Mamba	1.8	<b>97.2</b>	<b>94.3</b>	<b>3.2</b>

clean and noisy environments, highlighting its robustness in handling noise and reverberation. With the highest accuracy in 10° (96.9%), 15° (98.9%) and lowest MAE (2.5) in clean conditions, TF-Mamba outperforms FN-SSL. Although FN-SSL also analyzes direct-path features, TF-Mamba captures time and frequency dependencies more effectively, leading to better accuracy and robustness in challenging environments. In contrast, methods like SALSA-Lite, which processes noisy IPD with magnitude spectrum, and Cross3D, which uses the SRP-PHAT spatial spectrum, show significant performance drops under noise, underscoring the advantage of TF-Mamba.

### C. Results on real-world data

The results on the LOCATA dataset are presented in Table III, where the models trained on simulated data are directly tested. We observe that TF-Mamba achieves the best performance, with the highest accuracy at both 15° (97.2%) and 10° (94.3%) error tolerances, and the lowest MAE (3.2). This dataset’s relatively good acoustic conditions, which are almost noise-free and have an RT60 of 0.55s, allow all models to perform well. However, TF-Mamba’s superior accuracy and lower error indicate its ability to better capture fine localization details compared to the other methods. Notably, methods like SE-ResNet and SALSA-Lite, which are more complex in terms of parameters, show higher MAE, while simpler models like SELDnet struggle with accuracy and MAE. TF-Mamba’s approach also avoids the over-smoothing problem seen in other models during sudden sound source turns, maintaining strong localization performance in real-world conditions.

## VI. CONCLUSION

In this paper, we introduced TF-Mamba, a novel architecture for SSL that leverages the Mamba SSM to fuse time and frequency features effectively. By replacing traditional LSTM blocks with bidirectional Mamba, TF-Mamba enhances the modeling of audio sequence contexts while maintaining computational efficiency. Our experimental results, conducted on both simulated and real-world datasets, demonstrate that TF-Mamba significantly outperforms existing state-of-the-art methods. These findings highlight the potential of SSM like Mamba in advancing SSL tasks, marking the first application of such models in this field.

## VII. ACKNOWLEDGEMENT

The authors would like to thank Yabo Wang et. al. (The authors of FN-SSL [18]) for their valuable suggestions during this work on reproducing the FN-SSL model and other baseline models.

## REFERENCES

- [1] P.-A. Grumiaux, S. Kitić, L. Girin, and A. Guérin, "A survey of sound source localization with deep learning methods," *The Journal of the Acoustical Society of America*, vol. 152, no. 1, pp. 107–151, 07 2022.
- [2] P. Chiariotti, M. Martarelli, and P. Castellini, "Acoustic beamforming for noise source localization—Reviews, methodology and applications," *Mechanical Systems and Signal Processing*, vol. 120, pp. 422–448, 2019.
- [3] Z. Zhang, Y. Xu, M. Yu, S.-X. Zhang, L. Chen, and D. Yu, "ADL-MVDR: All deep learning MVDR beamformer for target speech separation," in *Proc. IEEE International Conference on Acoustics, Speech and Signal Processing (ICASSP)*, 2021, pp. 6089–6093.
- [4] Y. Xiao and R. K. Das, "Dual Knowledge Distillation for Efficient Sound Event Detection," in *International Conference on Acoustics, Speech and Signal Processing (ICASSP)*. IEEE, 2024.
- [5] H.-Y. Lee, J.-W. Cho, M. Kim, and H.-M. Park, "DNN-based feature enhancement using DOA-constrained ICA for robust speech recognition," *IEEE Signal Processing Letters*, vol. 23, no. 8, pp. 1091–1095, 2016.
- [6] A. Xenaki, J. Bünsow Boldt, and M. Græsbøll Christensen, "Sound source localization and speech enhancement with sparse bayesian learning beamforming," *The Journal of the Acoustical Society of America*, vol. 143, no. 6, pp. 3912–3921, 2018.
- [7] M. Raspaud, H. Viste, and G. Evangelista, "Binaural source localization by joint estimation of ILD and ITD," *IEEE Transactions on Audio, Speech, and Language Processing*, vol. 18, no. 1, pp. 68–77, 2009.
- [8] W. Zhang and B. D. Rao, "A two microphone-based approach for source localization of multiple speech sources," *IEEE Transactions on Audio, Speech, and Language Processing*, vol. 18, no. 8, pp. 1913–1928, 2010.
- [9] R. Schmidt, "Multiple emitter location and signal parameter estimation," *IEEE Transactions on Antennas and Propagation*, vol. 34, no. 3, pp. 276–280, 1986.
- [10] T. N. T. Nguyen, D. L. Jones, K. N. Watcharasupat, H. Phan, and W.-S. Gan, "SALSA-Lite: A fast and effective feature for polyphonic sound event localization and detection with microphone arrays," in *Proc. IEEE International Conference on Acoustics, Speech and Signal Processing (ICASSP)*, 2022.
- [11] A. Politis, K. Shimada, P. Sudarsanam, S. Adavanne, D. Krause, Y. Koyama, N. Takahashi, S. Takahashi, Y. Mitsufoji, and T. Virtanen, "STARSS22: A dataset of spatial recordings of real scenes with spatiotemporal annotations of sound events," in *Proc. the Detection and Classification of Acoustic Scenes and Events Workshop (DCASE)*, 2022, pp. 125–129.
- [12] Y. Xiao and R. K. Das, "Configurable DOA Estimation using Incremental Learning," *arXiv preprint:2407.03661*, 2024.
- [13] D. Suvorov, R. Zhukov, and G. Dong, "Deep residual network for sound source localization in the time domain," *Journal of Engineering and Applied Sciences*, vol. 13, no. 13, pp. 5096–5104, 2018.
- [14] B. Yang, H. Liu, and X. Li, "SRP-DNN: Learning direct-path phase difference for multiple moving sound source localization," in *Proc. IEEE International Conference on Acoustics, Speech and Signal Processing (ICASSP)*, 2022, pp. 721–725.
- [15] N. Ma, T. May, and G. J. Brown, "Exploiting deep neural networks and head movements for robust binaural localization of multiple sources in reverberant environments," *IEEE Transactions on Audio, Speech, and Language Processing*, vol. 25, no. 12, pp. 2444–2453, 2017.
- [16] S. Adavanne, A. Politis, and T. Virtanen, "Direction of arrival estimation for multiple sound sources using convolutional recurrent neural network," in *Proc. IEEE 26th European Signal Processing Conference (EUSIPCO)*, 2018, pp. 1462–1466.
- [17] C. Knapp and G. Carter, "The generalized correlation method for estimation of time delay," *IEEE Transactions on Acoustics, Speech, and Signal Processing*, vol. 24, no. 4, pp. 320–327, 1976.
- [18] Y. Wang, B. Yang, and X. Li, "FN-SSL: Full-band and narrow-band fusion for sound source localization," in *Proc. Interspeech*, 2023, pp. 3779–3783.
- [19] A. Gu, K. Goel, and C. Re, "Efficiently modeling long sequences with structured state spaces," in *Proc. International Conference on Learning Representations (ICLR)*, 2021.
- [20] A. Gu, K. Goel, A. Gupta, and C. Re, "On the parameterization and initialization of diagonal state space models," in *Proc. Advances in Neural Information Processing Systems (NIPS)*, vol. 35, 2022, pp. 35 971–35 983.
- [21] L. Zhu, B. Liao, Q. Zhang, X. Wang, W. Liu, and X. Wang, "Vision mamba: Efficient visual representation learning with bidirectional state space model," *arXiv preprint:2401.09417*, 2024.
- [22] O. Lieber, B. Lenz, H. Bata, G. Cohen, J. Osin, I. Dalmedigos, E. Safahi, S. Meirum, Y. Belinkov, S. Shalev-Shwartz, et al., "Jamba: A hybrid transformer-mamba language model," *arXiv preprint:2403.19887*, 2024.
- [23] K. Li and G. Chen, "Spmamba: State-space model is all you need in speech separation," *arXiv preprint:2404.02063*, 2024.
- [24] X. Jiang, C. Han, and N. Mesgarani, "Dual-path mamba: Short and long-term bidirectional selective structured state space models for speech separation," *arXiv preprint:2403.18257*, 2024.
- [25] R. Chao, W.-H. Cheng, M. La Quatra, S. M. Siniscalchi, C.-H. H. Yang, S.-W. Fu, and Y. Tsao, "An investigation of incorporating mamba for speech enhancement," *arXiv preprint:2405.06573*, 2024.
- [26] C. Quan and X. Li, "Multichannel long-term streaming neural speech enhancement for static and moving speakers," *IEEE Signal Processing Letters*, pp. 1–5, 2024.
- [27] M. H. Erol, A. Senocak, J. Feng, and J. S. Chung, "Audio Mamba: Bidirectional State Space Model for Audio Representation Learning," *arXiv preprint:2406.03344*, 2024.
- [28] Y. Chen, J. Yi, J. Xue, C. Wang, X. Zhang, S. Dong, S. Zeng, J. Tao, L. Zhao, and C. Fan, "RawBMamba: End-to-end bidirectional state space model for audio deepfake detection," in *Proc. Interspeech*, 2024.
- [29] S. Shams, S. S. Dindar, X. Jiang, and N. Mesgarani, "SSAMBA: Self-Supervised Audio Representation Learning with Mamba State Space Model," *arXiv preprint:2405.11831*, 2024.
- [30] D. Diaz-Guerra, A. Miguel, and J. R. Beltran, "Robust sound source tracking using SRP-PHAT and 3D convolutional neural networks," *IEEE Transactions on Audio, Speech, and Language Processing*, vol. 29, pp. 300–311, 2020.
- [31] J. S. Kim, H. J. Park, W. Shin, and S. W. Han, "A robust framework for sound event localization and detection on real recordings," *Tech. Rep.*, 2022.
- [32] S. Adavanne, A. Politis, J. Nikunen, and T. Virtanen, "Sound event localization and detection of overlapping sources using convolutional recurrent neural networks," *IEEE Journal of Selected Topics in Signal Processing*, vol. 13, no. 1, pp. 34–48, 2018.
- [33] T. N. T. Nguyen, D. L. Jones, K. N. Watcharasupat, H. Phan, and W.-S. Gan, "SALSA-Lite: A fast and effective feature for polyphonic sound event localization and detection with microphone arrays," in *Proc. IEEE International Conference on Acoustics, Speech and Signal Processing (ICASSP)*. IEEE, 2022, pp. 716–720.
- [34] A. Gu and T. Dao, "Mamba: Linear-time sequence modeling with selective state spaces," *arXiv preprint:2312.00752*, 2023.
- [35] G. Huang, Z. Liu, L. Van Der Maaten, and K. Q. Weinberger, "Densely connected convolutional networks," in *Proc. IEEE Conference on Computer Vision and Pattern Recognition (CVPR)*, 2017, pp. 4700–4708.
- [36] W. He, P. Motlicek, and J.-M. Odobez, "Neural network adaptation and data augmentation for multi-speaker direction-of-arrival estimation," *IEEE Transactions on Audio, Speech, and Language Processing*, vol. 29, pp. 1303–1317, 2021.
- [37] V. Panayotov, G. Chen, D. Povey, and S. Khudanpur, "Librispeech: an asr corpus based on public domain audio books," in *Proc. IEEE International Conference on Acoustics, Speech and Signal Processing (ICASSP)*, 2015, pp. 5206–5210.
- [38] D. Diaz-Guerra, A. Miguel, and J. R. Beltran, "gpuRIR: A python library for room impulse response simulation with GPU acceleration," *Multimedia Tools and Applications*, vol. 80, no. 4, pp. 5653–5671, 2021.
- [39] A. Varga and H. J. Steeneken, "Assessment for automatic speech recognition: II. NOISEX-92: A database and an experiment to study the effect of additive noise on speech recognition systems," *Speech communication*, vol. 12, no. 3, pp. 247–251, 1993.
- [40] E. A. Habets, I. Cohen, and S. Gannot, "Generating nonstationary multisensor signals under a spatial coherence constraint," *The Journal of the Acoustical Society of America*, vol. 124, no. 5, pp. 2911–2917, 2008.
- [41] H. W. Löllmann, C. Evers, A. Schmidt, H. Mellmann, H. Barfuss, P. A. Naylor, and W. Kellermann, "The LOCATA challenge data corpus for acoustic source localization and tracking," in *Proc. IEEE 10th Sensor Array and Multichannel Signal Processing Workshop (SAM)*. IEEE, 2018, pp. 410–414.
- [42] A. Brutti, L. Cristoforetti, W. Kellermann, L. Marquardt, and M. Omologo, "WOZ acoustic data collection for interactive TV," *Language Resources and Evaluation*, vol. 44, pp. 205–219, 2010.